# Effects of the microstructural uncertainties on the poroelastic and the diffusive properties of mortar

Adrien Socié, Yann Monerie, Frederic Perales

# Effects of the microstructural uncertainties on the poroelastic and the diffusive properties of mortar

🟢 Adrien SOCIÉ[1,3], 🟢 Yann MONERIE[2,3], and 🟢 Frédéric PERALES[1,3]

[1] Institut de Radioprotection et de Sureté Nucléaire (IRSN), PSN-RES/SEMIA/LSMA, BP3, Saint-Paul-lez-Durance, 13115, France
[2] Laboratoire de Mécanique et Génie Civil, University of Montpellier, CNRS, Montpellier, France
[3] MIST Laboratory, University of Montpellier, CNRS, IRSN, France

The assessment of the durability of civil engineering structures subjected to several chemical attacks require the development of chemo-poromechanical model. The mechanical and chemical degradations depend on several factors such as the initial composition of the porous medium. A multi-scale model is used to incorporate the multi-level microstructural properties of the mortal material. The present paper aims to study the effect of morphological and local material properties uncertainties on the poroelastic and diffusive properties of mortar estimated with the help of analytical homogenization. At first, the proposed model is validated for different cement paste and mortar by comparison to experimental results and micromechanical models. Secondly, based on a literature study, sensitivity and uncertainty analyses have been developed to assess the stochastic predictions of the multi-scale model. The main result highlights the predominant impact of the cement matrix phases (C-S-H) and interfacial transition area at the mortar scale. Furthermore, the sensitive analyses underline the material properties induce more variability than the volume fraction.

## 1    Introduction

The behavior of concrete is a topic of great concern in the context of the durability of civil engineering structures. The solicitations induced by the environment lead to the mineralogical evolution and delayed deformation of the concrete. The kinetic and the amplitude of the degradation depend on the properties and the mineralogy of the mature cementitious material. For example, several works bring out the effect of initial water cement ratio on the concrete delayed deformation and chemical reactions, such as for sulfate attack (El Hachem et al. 2012; Planel et al. 2006; Socie 2019), calcium leaching (Heukamp 2003; Stora et al. 2009) or drying shrinkage (Tognevi 2012). The water-cement ratio affects the cement paste composition and its porosity and thus modifies the overall poroelastic and diffusive properties of the material.

To consider the effect of the morphological multi-scale properties on the mechanical and chemical response of concrete under different loading, analytical and numerical models have been developed (Stora et al. 2009; Socié et al. 2022). The material properties of mature concrete based on multiscale models are performed in two steps: first, the morphological properties are estimated, second a micromechanics model is developed (Bary 2008; Bernard et al. 2012; Honorio et al. 2016; Göbel et al. 2017; Stora et al. 2009; Socié et al. 2022; Venkovic et al. 2013). At cement scale, the microstructure is estimated by hydration model (Bary 2008; Honorio et al. 2016; Göbel et al. 2017; Stora et al. 2009; Venkovic et al. 2013) and at mortar or concrete scale, an additional function is considered to estimate the volume fraction of the so-called Interfacial Transition Zone (ITZ) between the matrix and the inclusions (Garboczi et al. 1997; Honorio et al. 2016). Each model depends on a wide variety of parameters (the size of the inclusion, clinker composition...) that affect the estimated volume fraction and thus the macroscopic value (Honorio et al. 2016; Göbel et al. 2017; Venkovic et al. 2013). Furthermore, multi-scale models are function of the material properties of each phase considered. These properties are dependent on the experimental measurement (Constantinides et al. 2004; Haeckerd et al. 2005) and on the post-processing used (i.e. inverse analysis) (Hashin et al. 2002; Seigneur et al. 2017).

Therefore, a large number of parameters are required and their inherent uncertainty influences the predicted overall properties. Uncertainty and sensitivity analyses have already been carried out to quantify the stochastic variation due to hydration model and material properties from nanoscale to macroscale (concrete) (Göbel et al. 2017; Sudret et al. 2010; Venkovic et al. 2013). Göbel et al. (2017) reveal the uncertainty due to the input parameters is magnified during the upscaling processes and inclusion uncertainties take a major role in the overall elastic variation. Göbel et al. (2017) and Venkovic et al. (2013) determine the overall uncertainties of the hydration processes through the effects of the parameters. Göbel et al. (2017) show the effect of the hydration model uncertainties increases with the input parameter number. Göbel et al. (2017) and Venkovic et al. (2013) highlight that the elastic parameters have the major

contribution on the variability of the homogenized poroelastic properties. These works mostly focus on the elastic properties except (Venkovic et al. 2013) who have studied the poroelastic properties but only at the cement scale.

To our knowledge, no detailed study on the propagation of uncertainty of poroelastic and diffusion coefficients at the mortar scale have been carried out in the literature. Furthermore, besides the remarks of (Honorio et al. 2016) no study considers the influence of the ITZ uncertainties on the overall properties. The model developed in this study allows to estimate the poroelastic and diffusive properties of mortar used to simulate the chemo-poromechanical behavior of concrete submitted to chemical attacks (Socié et al. 2021; Socié et al. 2022). The paper is dedicated to the study of the impact of morphologic and material properties uncertainty on the poroelastic and diffusive efficient coefficients of mortar estimated by analytical homogenization.

This paper begins with a description of the microporomechanics model (Section 2). The Section 3 is dedicated to its validation. The impact of the main variable in the homogenized value is underlined. The uncertainties of the microstructural and morphological parameters are studied in the Section 4. At first, each uncertainty is studied separately to exhibit the main input parameters factor. The study highlights the main effect of the cement paste matrix, C-S-H, and ITZ to respectively the cement paste and mortar variation. Secondly, the global uncertainties are presented for three mortars distinguish by their water-cement ratios: 0.3, 0.4 and 0.5. The main results show the uncertainty increases with the upscaling and the predominant impacts of the ITZ characteristic on the chemo-mechanical mortar properties. A Sobol variance decomposition is studied in the Section 5 to highlight the impact of the main input variable and their interactions.

## 2   Microporomechanical model

The multi-scale model permits to identify the poroelastic parameters and the diffusion coefficient of the chemo-poromechanical model developed in (Socié et al. 2022; Socie 2019). The model is dedicated to the study of geomaterial expansion due to the strong precipitation of a solid inside the porous medium. The chemical software describes the mineralogy evolution and the poromechanical model estimates the swelling by the volume fraction of the main precipitated solid, denoted $\varphi_{ms}$. The porous medium is described with an isotropic elastic poromechanical model, where the pressure depends on the volume fraction of the main precipitated solid and the strain tensor (Socié et al. 2022):

$$\begin{cases} \sigma = \mathbb{C} : \varepsilon - bP\mathbf{I} \\ P = N \left\langle \varphi_{ms} - \left\langle \varphi_{ms}^0 + btr(\varepsilon) \right\rangle_+ \right\rangle_+, \end{cases} \tag{1}$$

where $\sigma$ is the Cauchy stress tensor [Pa] , $\mathbb{C}$ is the fourth order stiffness tensor [Pa], $\varepsilon$ is the linearized strain tensor, $P$ is the pore pressure [Pa], $\mathbf{I}$ is the identity second order tensor, $b$ is the Biot coefficient assuming overall isotropy [−], $N$ is the Biot skeleton modulus [Pa], $\langle x \rangle_+ = (x + |x|)/2$ are the Macaulay brackets, and $\varphi_{ms}^0$ represents the quantity of initial pores to be filled by the solid to induce swelling [−].

The microporomechanical model aims to estimate the following mortar variables from the microstructure:

- Biot coefficient $b_m$ and Biot skeleton modulus $N_m$,
- bulk and shear modulus, $k_m$ and $g_m$, Young modulus $E_m$ and Poisson coefficient $v_m$,
- diffusion coefficient $D_m$.

The subscript $m$ defines the phase of the mortar material. The Biot parameters are obtained considering the main precipitated solid phases in the capillary pores and the porosity of the mortar's Interfacial Transition Zone.

The following sections describe the homogenization function (Section 2.2) based on a multi-scale representativity (Section 2.1).

### 2.1   Description of the mortar microstructure

We consider two-scale modeling (Figure 1):

1. Level I: cement paste. The cement paste is a material with an isotropic matrix, called C-S-H, containing inclusions randomly distributed in space and in orientation. The inclusions correspond to the main solid hydrated phases (Socié et al. 2022; Socié et al. 2021): portlandite, ettringite, and katoite.
2. Level II: mortar scale. Mortar is a three coated with an isotropic matrix (cement paste) containing inclusions randomly distributed in space and in orientation (sand) and a percolation phase called the Interfacial Transition Zone (ITZ).

The C-S-H  phase can be described as a porous medium with two types of C-S-H. The C-S-H  density impacts mechanical and diffusive properties (Bejaoui et al. 2007; Constantinides et al. 2004; Stora et al. 2009; Tennis et al. 2000; Ulm et al. 2004) and some models have different cement paste representations or

consider a dedicated representation for the C-S-H scale (Bary et al. 2014; Béajoui et al. 2006; Honorio et al. 2016; Göbel et al. 2017; Venkovic et al. 2013; Ulm et al. 2004). Furthermore, some studies (Honorio et al. 2016; Stora et al. 2009) consider a representation of the ITZ phase whereas (Hashin et al. 2002; Heukamp 2003) estimate its properties from the cement paste value. Because of the microstructure and the associated coefficients of C-S-H and ITZ are difficult to obtain, we choose to not describe their microstructures. Their coefficients are obtained with a probabilistic distribution function.
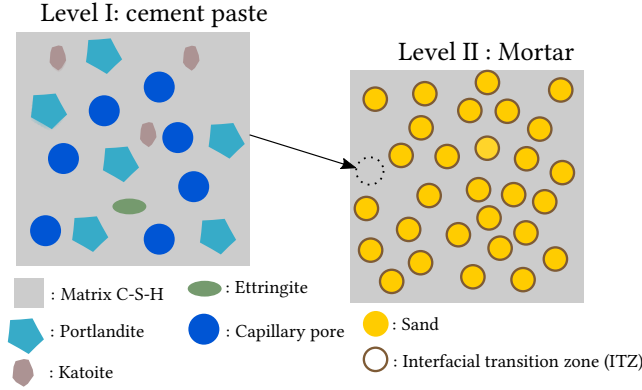


**Figure 1:** Representation of multiscale heterogeneous microstructure of mortar.

## 2.2 Estimation of the chemo-poromechanical properties

The homogenization schemes follow the recommendations of the literature and are similar for mechanical and diffusive properties:

1. Cement paste: Mori-Tanaka scheme (Mori et al. 1973) used in (Bary 2008; Heukamp 2003; Venkovic et al. 2013; Ulm et al. 2004; Le 2011),
2. Mortar: General Self-Consistent scheme (Hashin et al. 2002) used in (Bary et al. 2006; Tognevi 2012; Stora et al. 2009).

### 2.2.1 Cement paste

The cement paste is assumed to be composed of $N^{ph}$ phases: $N^{sol}$ solid phases and capillarity pores, contained in a matrix of C-S-H. We consider a spherical distribution of each inclusion and pore. The bulk $k_{cp}$ and shear $g_{cp}$ moduli depend on the volume fraction $\varphi_i$, shear modulus $g_i$ and bulk modulus $k_i$ of the phase $i$ such that:

$$
\begin{cases}
k_{cp} = \dfrac{k_{csh} + \dfrac{4g_{csh}}{3}\displaystyle\sum_{i=1}^{N^{ph}} \varphi_i \dfrac{k_i - k_{csh}}{k_i + 4/3g_{csh}}}{1 - \displaystyle\sum_{i=1}^{N^{ph}} \varphi_i \dfrac{k_i - k_{csh}}{k_i + 4/3g_{csh}}} \quad g_{cp} = \dfrac{g_{csh} + H_{csh}\displaystyle\sum_{i=1}^{N^{ph}} \varphi_i \dfrac{g_i - g_{csh}}{g_i + H_{csh}}}{1 - \displaystyle\sum_{i=1}^{N^{ph}} \varphi_i \dfrac{g_i - g_{csh}}{g_i + H_{csh}}} \\[3em]
H_{csh} = \dfrac{g_{csh}\left(3/2k_{csh} + 4/3g_{csh}\right)}{k_{csh} + 2g_{csh}},
\end{cases}
\tag{2}
$$

where the subscripts *csh* and *cp* denote C-S-H and cement paste respectively.

We only consider the main precipitated solid in the capillarity porosity and ITZ porosity (Socié et al. 2021; Socie 2019) and not the C-S-H's poroelastic properties. In that way, the Biot tensor $b_{cp}\mathbf{I}$ and Biot skeleton modulus $N_{cp}$ of the cement paste only depend on the hydrostatic part of the localization tensor $A_i^h$ (Ulm et al. 2004):

$$
\begin{cases}
b_{cp}\mathbf{I} = \left[\left(1 - \displaystyle\sum_{i=1}^{N^{sol}} \varphi_i A_i^h\right)\right]\mathbf{I}, \qquad \dfrac{1}{N_{cp}} = \displaystyle\sum_{i=1}^{N^{sol}} \dfrac{\varphi_i \left(1 - A_i^h\right)}{k_i} \\[2em]
A_i^h = \left(1 + \dfrac{3k_{csh}}{3k_{csh} + 4g_{csh}}\left(\dfrac{k_i}{k_{csh}} - 1\right)\right)^{-1} \left[\displaystyle\sum_{i}^{N^{ph}} \varphi_i \left(1 + \dfrac{3k_{csh}}{3k_{csh} + 4g_{csh}}\left(\dfrac{k_i}{k_{csh}} - 1\right)\right)^{-1}\right]^{-1}.
\end{cases}
\tag{3}
$$

The effective diffusion coefficient $D_{cp}$ of the cement paste depends on the diffusion of the phases

(Dormieux et al. 2006):

$$D_{cp} = D_{csh} \frac{1 + 2\sum_i \varphi_i \dfrac{D_i - D_{csh}}{D_i + 2D_{csh}}}{1 - \sum_i \varphi_i \dfrac{D_i - D_{csh}}{D_i + 2D_{csh}}}. \tag{4}$$

Moreover, we assume that the capillary porosity and the C-S-H are the only diffusive phases (Bary et al. 2014; Bary et al. 2006; Bogdan 2015; Stora et al. 2009).

### 2.2.2   Mortar

The mortar is mainly represented as a three-coated sphere assemblage where the General Self-Consistent scheme is used in order to take into account a percolation of the ITZ phase (Bary et al. 2006). The mortar properties depend on the ITZ, the sand and the cement paste properties. In this section, the subscript *itz* and *s* respectively define the ITZ and sand. The bulk property is defined by (Hashin et al. 2002; Nguyen et al. 2011; Tognevi 2012) :

$$\begin{cases} k_m = k_{cp} + \dfrac{\varphi_s + \varphi_{itz}}{\dfrac{1}{k^* - k_{cp}} + \dfrac{3\varphi_{cp}}{3k_{itz} + 4g_{itz}}}, \\[20pt] k^* = k_{itz} + \dfrac{\varphi_s/(\varphi_s + \varphi_{itz})}{1/(k_s - k_{itz}) + 3\varphi_{itz}/(\varphi_s + \varphi_{itz})/(3k_{itz} + 4g_{itz})}. \end{cases} \tag{5}$$

The shear modulus is deduced from an implicit system depicted in (Hashin et al. 2002; Nguyen 2010; Socie 2019). For a sake of compactness, we refer the reader to these papers for details. The Biot coefficient and skeleton modulus depend on poroelastic phases values (Bary et al. 2006; Nguyen et al. 2011) :

$$\begin{cases} b_m = b_{cp} + \\[6pt] \dfrac{(3k_{cp} + 4g_{cp})(1 - \varphi_{cp})\left[(b_{itz} - b_{cp})(4g_{itz}(1 - \varphi_{cp}) + 3k_1^*) - \varphi_s(b_{itz} - 1)(3k_{itz} + 4g_{itz})\right]}{9k_s k_{itz}\varphi_{cp}(1 - \varphi_{cp}) + 12g_{itz}k_2^*\varphi_{cp} + (4g_{cp} + 3k_{cp}(1 - \varphi_{cp}))(4g_{itz}(1 - \varphi_{cp}) + 3k_1^*)}, \\[10pt] \text{with } k_1^* = k_{itz}\varphi_s + k_s\varphi_{itz} \text{ and } k_2^* = k_s\varphi_s + k_{itz}\varphi_{itz}. \end{cases} \tag{6}$$

$$\begin{cases} \dfrac{1}{N_m} = \dfrac{\varphi_s + \varphi_{itz}}{N^*} + \dfrac{\varphi_{cp}}{N_{cp}} + \dfrac{(b^* - b_{cp})^2 \varphi_s(\varphi_s + \varphi_{itz})}{3(\varphi_s + \varphi_{itz})(k_{cp} - k^*) + 3k^* + 4g_{cp}} \\[14pt] \dfrac{1}{N^*} = \dfrac{\varphi_s/(\varphi_s + \varphi_{itz})}{N_s} + \dfrac{1 - \varphi_s/(\varphi_s + \varphi_{itz})}{N_{itz}} \\[6pt] \qquad + \dfrac{3(b_{itz} - b_s)^2(1 - \varphi_s/(\varphi_s + \varphi_{itz}))\varphi_s/(\varphi_s + \varphi_{itz})}{3\varphi_s(k_{itz} - k_s)/(\varphi_s + \varphi_{itz}) + 3k_s + 4g_{itz}} \\[14pt] b^* = b_{itz} + \dfrac{(3k_{itz} + 4g_{itz})(b_m - b_{itz})\varphi_s/(\varphi_s + \varphi_{itz})}{4g_{itz} + 3k_s(1 - \varphi_s/(\varphi_s + \varphi_{itz}) + 3k_{itz}\varphi_s/(\varphi_s + \varphi_{itz}))}. \end{cases} \tag{7}$$

The sand is considered nonreactive with a negligible diffusion coefficient. Based on the works of (Bogdan 2015; Heukamp 2003; Hashin et al. 2002; Salah et al. 2019), elastic and diffusive properties of ITZ are deduced from the cement paste coefficients. As a first approach, due to the high porosity of ITZ phase and because the phase is mostly composed of matrix solid phases (Honorio et al. 2016), the poroelastic properties of the ITZ are estimated from a bimaterial representation (Dormieux et al. 2006):

$$b_{itz} = 1 - \frac{k_{itz}}{k_{csh}}; \qquad\qquad \frac{1}{N_{itz}} = \frac{b_{itz} - \phi_{itz}}{k_{csh}}. \tag{8}$$

The diffusive coefficient of the mortar is estimated with the so-called three-coated sphere model (Bary et al. 2006; Stora et al. 2009):

$$\begin{cases} D_m = D_{cp} + (1 - \varphi_{cp})\left[\left[D_{itz} - D_{cp} + D_1^*\left(D_2^*\right)^{-1}\right]^{-1} + \dfrac{\varphi_{cp}}{3D_{cp}}\right]^{-1}, \\[12pt] \text{with } D_1^* = \dfrac{\varphi_s}{\varphi_s + \varphi_{itz}} \text{ and } D_2^* = (D_s - D_{itz})^{-1} + \left(1 - D_1^*\right)(3D_{itz})^{-1}. \end{cases} \tag{9}$$

# 3   Validation

This section aims to validate this simple and closed-form model by comparison with a more sophisticated model (Stora et al. 2009) and the model's availability to capture the microstructure variation.

## 3.1   Impact of the microstructure evolution

The ability of the model to describe the microstructure evolution is depicted with the effect of the water-cement mass ratio on the overall properties. The cement paste microstructure is estimated by (Bary et al. 2006; Tognevi 2012) and summarized in the Table 1. The material properties are described in the Table 2. The mechanical results agree well with the experimental measurements of (Haeckerd et al. 2005) (cf. Figure 2(a)).

| $w/c$ | Ettringite | Katoite | Portlandite | Anhydrate | C-S-H |
|-------|-----------|---------|-------------|-----------|-------|
| 0.3   | 0.074     | 0.072   | 0.152       | 0.137     | 0.494 |
| 0.35  | 0.075     | 0.072   | 0.156       | 0.094     | 0.507 |
| 0.4   | 0.072     | 0.073   | 0.155       | 0.064     | 0.509 |
| 0.45  | 0.069     | 0.073   | 0.151       | 0.043     | 0.504 |
| 0.5   | 0.065     | 0.075   | 0.144       | 0.03      | 0.494 |
| 0.6   | 0.058     | 0.068   | 0.131       | 0.014     | 0.48  |

**Table 1:** Cement paste composition (Bary et al. 2006; Tognevi 2012).

|  | $D$ [m$^2$ s$^{-1}$] | $E$ [GPa] | $\nu$ | References |
|---|---|---|---|---|
| C-S-H | $7.24 \times 10^{-12}$ | 23.8 | 0.24 | (Constantinides et al. 2004; Venkovic et al. 2013) and Table 12 |
| Portlandite | 0 | 38 | 0.324 | (Haeckerd et al. 2005; Venkovic et al. 2013) |
| Ettringite, Katoite | 0 | 22.4 | 0.25 | (Haeckerd et al. 2005) |
| Anhydrous cement | 0 | 117.6 | 0.314 | (Haeckerd et al. 2005) |
| Sand | 0 | 62.4 | 0.21 | (Heukamp 2003) |
| Capillary pore | $D_0 = 2 \times 10^{-9}$ | 0 | 0 | (Bogdan 2015) |
| ITZ | $10.3 D_{cp}$ | $0.175 \times E_{cp}$ | $\nu_{cp}$ | Table 13 and Table 14 |

**Table 2:** Material properties of mortar phases.

The diffusion coefficient is compared to the experimental results described in (Bary et al. 2006) (cf. Figure 2(b)). The C-S-H diffusion coefficient used is equal to $8 \times 10^{-12}$ m$^2$ s$^{-1}$ to fit the experimental result. The diffusion model can catch the effects of the microstructure and fit well the experimental results. Nevertheless, for low water-cement ratio, the model overestimates the diffusion value due to the simplified representation of the C-S-H phases. As described in (Bary et al. 2006), the model needs to consider the influence of the water-cement ratio in the volume fraction of C-S-H phases.
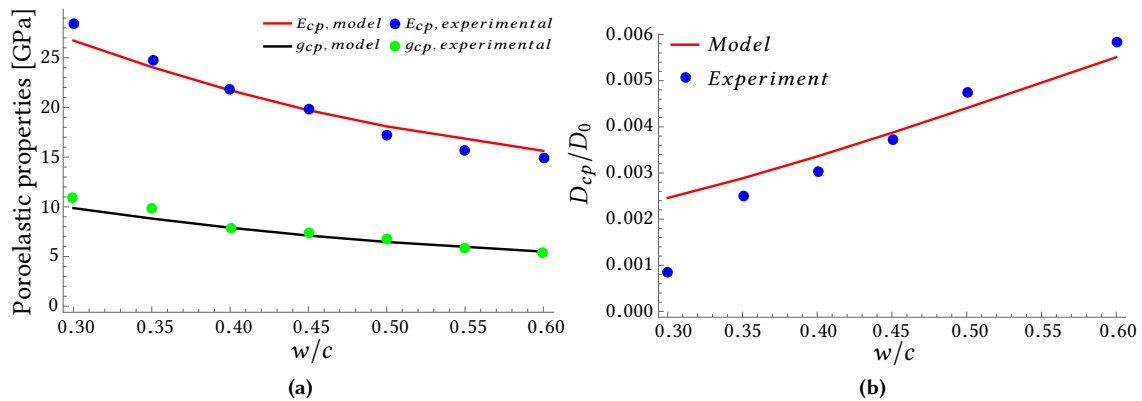


**Figure 2:** Effect of the water-cement ratio ($w/c$) on the material properties of cement paste: a) elastic properties compared to (Haeckerd et al. 2005) and b) normalized diffusion properties compared to (Bary et al. 2006).

## 3.2    Validation of the Micromechanical representation

In the Table 3, the model is compared to the reference model of Stora et al. (2009) which have a microstructure representation of the C-S-H and the ITZ phases. The microstructure and the hydrated properties are taken from (Stora et al. 2009). The range of values are estimated using a Monte Carlo experiments on 10000 samples to take into account the uncertainties associated with the C-S-H and ITZ properties (see Table 2 and Table 4). The diffusion and elastic properties fit well with the model and experimental results, except for the material (Gallé et al. 2004) where the model estimates a lower Young's modulus value.

| Material | Parameters | Model | (Stora et al. 2009) | Experimental results |
|---|---|---|---|---|
| Cement paste (Gallé et al. 2004) | Young Modulus [GPa] | $20.389 \pm 1.1$ | 23.7 | 23. |
| Cement paste (Le Bellego 2001) | Young Modulus [GPa] | $23.58 \pm 1.27$ | 25.65 | |
| | Diffusion coefficient $(10^{-12})$ $[\mathrm{m^2\,s^{-1}}]$ | $3.02 \pm 1.44$ | 3.2 | |
| Mortar (Le Bellego 2001) | Young Modulus [GPa] | $39.45 \pm 3.44$ | 38.5 | 38.2 |
| | Diffusion coefficient $(10^{-12})$ $[\mathrm{m^2\,s^{-1}}]$ | $3.33 \pm 1.95$ | 1.8 | 1.7 |

**Table 3:** Comparison of the micromechanical estimation of cement paste and mortar properties with experimental data (Le Bellego 2001; Gallé et al. 2004) and analytical homogenization model (Stora et al. 2009).

**Main results**    The model can both predict the poroelastic and diffusive properties from an estimated microstructure and capture the effects of the cement mineralogy in the overall behavior.

# 4    Uncertainty propagation

The propagation of uncertainty of the poroelastic and diffusive mortar properties are studied through a Monte Carlo method. At first, each uncertainty is studied separately and divided into two domains: material properties (Section 4.1) and microstructural characteristics (Section 4.2). We consider a mortar composed of a CEM I cement paste (see Table 1) with a water-cement ratio of 0.4, an ITZ volume fraction of 0.185 and a volume fraction of sand of 0.55. Each parameter is studied and the others are taken equal to their mean values (see Table 1 and Table 2). Secondly, we study the impact of the global uncertainties for three water-cement ratios: 0.3, 0.4 and 0.5.

A Monte-Carlo study with 10000 simulations by parameter is performed. In the sequel, the input parameters of the multi-scale model are described by log-normal distributions to ensure the strict positivity:

$$p(x) = \frac{1}{xV\sqrt{2\pi}} exp\left(-\left(\frac{ln(x) - \overline{e}}{V\sqrt{2}}\right)^2\right), \qquad (10)$$

where $\overline{e}$ and $V$ are the mean and the standard deviation of the normal law distribution. For each study, the output mean and standard deviation are estimated.

The appendices are dedicated to the estimation of the parameters uncertainties and sum up the different coefficients used in the literature.

## 4.1    Uncertainty from the material properties

### 4.1.1    Input parameters

**Solid uncertainties at cement paste scale**    At cement paste scale, the porous medium is affected by the uncertainties associated with the solid phases (hydrates). The global sensitivity analysis led by (Venkovic et al. 2013) have shown that the poroelastic properties are essentially impacted by the properties of C-S-H and portlandite. Based on the work of (Venkovic et al. 2013), we study the impact of the uncertainties of the Young Modulus of the two hydrates. For the diffusion part, the study is focused on the C-S-H phase. Indeed, in the analytical model benchmark led by (Patel et al. 2016), the authors highlight that every tested multi-scale and empirical model have to fit the diffusion associated with the matrix phases that induces a wide variability of values (see Appendix A.2). This wide variability is explained by the difference in the microstructure representation and the fact that the calibration value depends on the experimental techniques used to obtain the cement paste diffusivity (Patel et al. 2016). Furthermore, the C-S-H's diffusion coefficient is difficult to identify because of the sorption reactions between the cation and anion in solution and the solid phases (Seigneur et al. 2017).

**ITZ properties** At mortar scale, the ITZ value mainly affects the poroelastic and diffusion properties (Heukamp 2003; Honorio et al. 2016). The Table 13 and Table 14 show the large variability in the literature. The values are generally estimated by inverse analysis (Heukamp 2003; Hashin et al. 2002; Garboczi 1997; Patel et al. 2016) which depends both on the analytical homogenization/numerical scheme used and the experiment uncertainties (Aït-Mokhtar et al. 2013; Patel et al. 2016).

The input parameters are summed up in Table 4. The mean and the standard deviation of portlandite's Young modulus are identified from (Constantinides et al. 2004; Venkovic et al. 2013). The C-S-H value is estimated for water-cement ratios of 0.3 and 0.5 by analytical homogenization (Mori-Tanaka scheme) from the measurement of the uncertainties (Constantinides et al. 2004). The high and low-density C-S-H 's volume fraction are estimated from Tennis and Jennings' formula (Tennis et al. 2000). The mean and standard deviation of the C-S-H diffusion and ITZ properties are estimated from the literature respectively presented in the appendices A.2 and A.3.

| | $D_{csh}$ [m$^2$ s$^{-1}$] | $E_{csh}$ [GPa] | $E_{ch}$ [GPa] | $D_{itz}$ [m$^2$ s$^{-1}$] | $E_{itz}$ |
|---|---|---|---|---|---|
| V | $7.37 \times 10^{-12}$ | 2 | 5 | $6.93 \times D_{cp}$ | $0.175 \times E_{cp}$ |

**Table 4:** Input parameters, material properties uncertainties.

### 4.1.2 Results

The results are shown in Table 5 and plotted in Figure 3. At cement scale, the C-S-H has the main uncertainties impact. Contrary to the results of (Venkovic et al. 2013) and (Göbel et al. 2017), the portlandite and C-S-H elastic properties have not a strong impact on effective mortar properties. The mortar poroelastic properties are mainly affected by the uncertainties associated with the ITZ rigidity (strong input dispersion, see Table 14) and the poroelastic properties of the transition zone (Nguyen et al. 2011). The uncertainties propagation from cement paste to the mortar admit a quite similar variance.

The diffusion coefficient has a larger variance than the elastic properties. First of all, the C-S-H uncertainties have a significant effect on the mortar and cement paste properties. The uncertainty propagation is stable and the mortar standard deviation is larger than of the cement paste. This effect is undergone by the ITZ diffusion coefficient that is a function of the cement paste properties. At mortar level, the ITZ still plays a major role in the uncertainty.

| Uncertainties | $E_{cp}$ [GPa] | $E_m$ [GPa] | $b_m N_m$ [GPa] | $D_{cp}/D_0 \times 10^3$ | $D_m/D_0 \times 10^3$ |
|---|---|---|---|---|---|
| $E_{csh}$ | 21.36(±1.2) | 37.43(±1.01) | 25.07(±0.7) | – | – |
| $E_{ch}$ | 21.35(±0.4) | 37.45(±0.31) | 25.04(±0.56) | – | – |
| $E_{itz}/E_{cp}$ | – | 36.66(±5.01) | 26.42(±18.11) | – | – |
| $D_{csh}$ | - | - | - | 1.6(±0.76) | 2.6(±1.22) |
| $D_{itz}/D_{cp}$ | - | - | - | - | 4.65(±2.) |

**Table 5:** Impact of the material properties uncertainties on the homogenized properties.
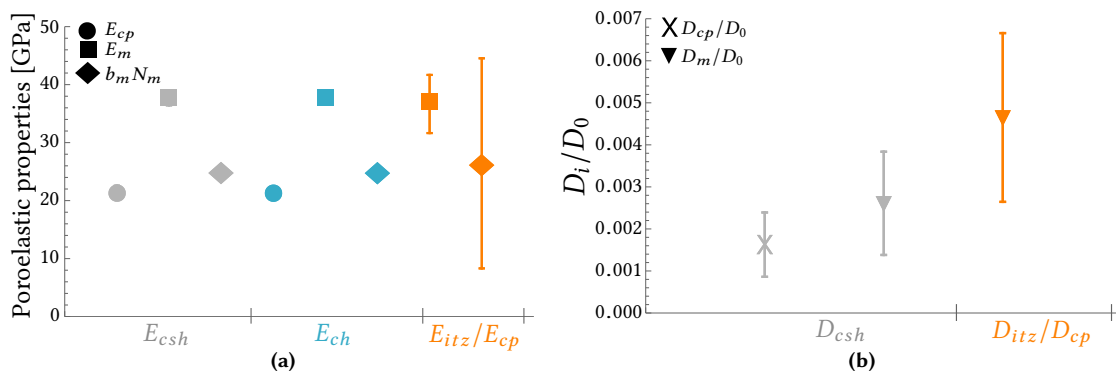


**Figure 3:** Results of the uncertainty propagation from the material properties, the mean and standard deviation obtained by the Monte Carlo simulation are respectively represented by the data symbol and the error bar: a) poroelastic properties and b) normalized diffusion properties.

**Main results** The C-S-H and ITZ have the main uncertainties impact respectively at cement paste and mortar scales. For only the diffusion, the C-S-H uncertainties play a major role in the global mortar variance.

## 4.2   Uncertainty from the microstructure

### 4.2.1   Input parameters

We consider two main impacts of the microstructure in each level: the hydrate volume fraction and the ITZ volume fraction.

**Hydrate volume fraction**   Most of the hydration models (Buffo-Lacarrière et al. 2007; Papadakis et al. 1991; Jennings et al. 1994; Tennis et al. 2000) are based on the alite, belite, aluminate and ferrite mass fractions estimated from the chemical clinker composition by the Bogue's formula (Bogue 1952). Stutzman et al. (2014) highlight that the Bogue constant introduces a significant uncertainties that mainly impacts the alite and belite mass fractions (around 10%) and thus the portlandite and C-S-H volume fractions. Furthermore, we notice a strong variability of C-S-H molar volume in the literature: for a calcium silica ratio of 1.65, the molar volume is equal to 0.084 $L.mol^{-1}$ (Planel 2002) or 0.078 $L.mol^{-1}$ (Lothenbach et al. 2019). This variability impacts the overall properties estimated by the hydration-homogenization model (Socie 2019). In order to capture both the impact of Bogue's constant and molar volume uncertainties in the microstructure properties, a Monte Carlo study is carried out using the hydration model of (Socie 2019; Socié et al. 2022) (see Appendix A.1). The associated standard deviations are applied to the studied microstructures (cf. Table 6). The variation of the solid volume fraction impacts the overall properties through the capillary porosity:

$$\phi = 1 - \sum_{i}^{N^{sol}} \varphi_i. \tag{11}$$

| | Cement paste level | | | | Mortar level | |
|---|---|---|---|---|---|---|
| | $\varphi_{csh}$ | $\varphi_{ch}$ | $\varphi_{ett}$ | $\varphi_{kat}$ | $\varphi_{itz}$ | $\phi_{itz}/\phi_{cp}$ |
| $V$ | 0.018 | 0.005 | 0.007 | 0.011 | 0.071 | 0.25 |

**Table 6:** Input parameters, the microstructural uncertainties. The subscript *kat* and *ett* respectively define the values associated with the katoite and ettringite.

**ITZ volume fraction**   The ITZ volume fraction depends on the sand granulometry (Garboczi et al. 1997), the sand mean size particle (Garboczi et al. 1997), the hydration rate (Sun et al. 2007), the inclusion properties (Keinde 2014) and the water cement ratio (Sun et al. 2007; Tognevi 2012). The ITZ volume fraction is usually estimated from the particle size distribution of sand and considering a constant ITZ thickness by the Garboczi's formula (Garboczi et al. 1997), such as (Heukamp 2003; Honorio et al. 2016; Stora et al. 2009; Tognevi 2012). The great uncertainty of ITZ thickness influences the estimation of the volume fraction (Honorio et al. 2016). The mean and the standard deviation are deduced from the volume fractions used in the literature (see Table 15). The variation of the ITZ volume fraction impacts the cement paste volume fraction such as:

$$\varphi_{cp} = 1 - \varphi_{itz} - \varphi_s. \tag{12}$$

Finally, to study the influence of the ITZ porosity on the poroelastic properties (8), an uncertainty analysis is carried out with the mean value of $\phi_{itz}/\phi$ equals to **1.75** and a standard deviation of **0.25** (based on the global values used in the literature, Table 16).

### 4.2.2   Results

The results are presented in the Table 7 and plotted in the Figure 4.

At cement paste scale, the variations of poroelastic properties and diffusion coefficient increase with the volume fraction uncertainties. This effect is due to two aspects. First of all, the Young modulus of each hydrate remains similar and we do not consider their diffusivity (cf. Table 2). Secondly, the porosity is linearly dependent on the volume fraction (11). The katoite is thus the phase with the more significant impact on the efficient variation properties. Note that the variation of the solid fraction of the aluminate phases can also impact the chemo-mechanical response (such as sulfate attack (Socié et al. 2022)). The matrix (C-S-H) remains the phases whose uncertainties has the more impact on the estimated properties.

At mortar scale, the mortar variation is, first of all, induced by the ITZ volume fraction uncertainty. Patel et al. (Patel et al. 2016) observe a low impact of the ITZ phase on the diffusion properties, which may call into question the main influence of the mortar homogenization scheme obtained. Furthermore, contrary to other schemes (Sanahuja et al. 2017; Stora et al. 2009), the Maxwell/Mori-Tanaka scheme (4) is not directly function of the volume fraction of the matrix phases. As Göbel et al. (2017), the uncertainty of the cement paste parameters is magnified during the upscaling processes but, for the elastic and diffusion coefficients, their influences are negligible compared to the ITZ uncertainty. The Biot properties are impacted by the porosity and the volume fraction of ITZ. Note that the ITZ porosity has been little studied in the literature that could have a strong impact on the overall properties (see Table 16).

| Uncertainties | $E_{cp}$ [GPa] | $E_m$ [GPa] | $b_m N_m$ [GPa] | $D_{cp}/D_0 \times 10^3$ | $D_m/D_0 \times 10^3$ |
|---|---|---|---|---|---|
| $\varphi_{csh}$ | 21.39(±0.78) | 37.46(±0.66) | 25.14(±2.03) | 1.64(±0.09) | 2.63(±0.15) |
| $\varphi_{ch}$ | 21.38(±0.26) | 37.47(±0.23) | 25.07(±0.44) | 1.64(±0.04) | 2.63(±0.06) |
| $\varphi_{ett}$ | 21.39(±0.29) | 37.48(±0.25) | 25.06(±0.78) | 1.64(±0.05) | 2.63(±0.09) |
| $\varphi_{kat}$ | 21.39(±0.46) | 37.48(±0.39) | 25.06(±1.23) | 1.64(±0.08) | 2.63(±0.14) |
| $\varphi_{itz}$ | – | 37.65(±2.76) | 24.91(±2.95) | – | 3.(±0.83) |
| $\phi_{itz}/\phi_{cp}$ | – | – | 25.26(±2.37) | – | – |

Table 7: Impact of the microstructural properties uncertainties on the homogenized properties.
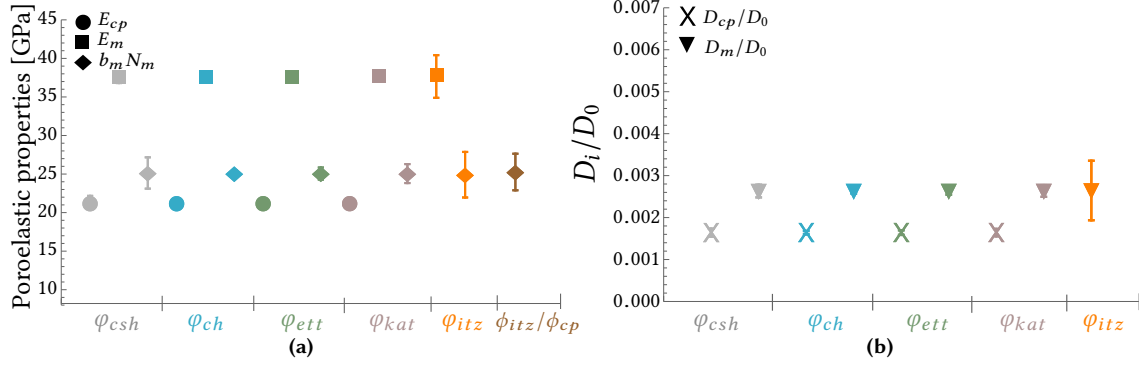


Figure 4: Results of the uncertainty propagation from the microstructural properties (volume fractions and porosities), the mean and standard deviation obtained by the Monte Carlo simulation are respectively represented by the data symbol and the error bar: a) poroelastic properties and b) normalized diffusion properties.

**Main results**     The variations of poroelastic properties and diffusion coefficient increase with the volume fraction uncertainties of the inclusion and theirs impacts are magnified during the upscaling processes. The main sources of uncertainty at the cement paste and mortar scales remain respectively the C-S-H and ITZ properties.

## 4.3    Impact of all uncertainties

The impacts of material and morphological uncertainties on the analytical estimated results are investigated. Based on the remarks of (Stutzman et al. 2014) regarding the uncertainties associated with the Bogue formula rendering "supposedly distinct classes of cement practically indistinguishable", the homogenization propagation uncertainties are studied for three water-cement ratios.

The evolution of the apparent material properties is shown in Table 8 and plotted in Figure 5. The mean parameters follow the tendencies specified in the literature (experimental, numerical and analytical results): the diffusion increases and the Young Modulus decreases with the water-cement ratio (Bary et al. 2006; Béajoui et al. 2006; Bernard et al. 2012; Patel et al. 2016; Tognevi 2012). As previous results, the uncertainties increase with the mortar parameters, in particular the diffusion coefficients. Furthermore, the Biot coefficient evolution with water-cement ratio is not clear.

| $w/c$ | $E_{cp}$ [GPa] | $E_m$ [GPa] | $b_m N_m$ [GPa] | $D_{cp}/D_0 \times 10^3$ | $D_m/D_0 \times 10^3$ |
|---|---|---|---|---|---|
| 0.3 | 23.34(±1.78) | 38.07(±6.54) | 30.14(±27.73) | 1.21(±0.58) | 1.88(±1.3) |
| 0.4 | 18.92(±1.51) | 34.39(±5.96) | 32.54(±23.03) | 1.64(±0.85) | 2.5(±2.1) |
| 0.5 | 15.66(±1.29) | 31(±5.68) | 38.22(±27.7) | 2.14(±1.) | 3.3(±2.3) |

Table 8: Input parameters, properties uncertainties study.

The standard deviation increases with the upscaling due to the propagation of the uncertainties through the ITZ properties and volume fraction. The dependency of the standard deviation value with the water-cement ratio is not clear due to the main impact of the material properties. The coefficient variation $(V/\overline{e})$ is mainly impacted by the water-cement ratio and so for a low water-cement ratio, the predicted values admit a small error.

## 5    Sensitivity analysis

The Section 4 highlights the impact of the morphologic and the material properties parameters in the global response. To identify the main contributor to the output variation, a sensitivity analysis study is
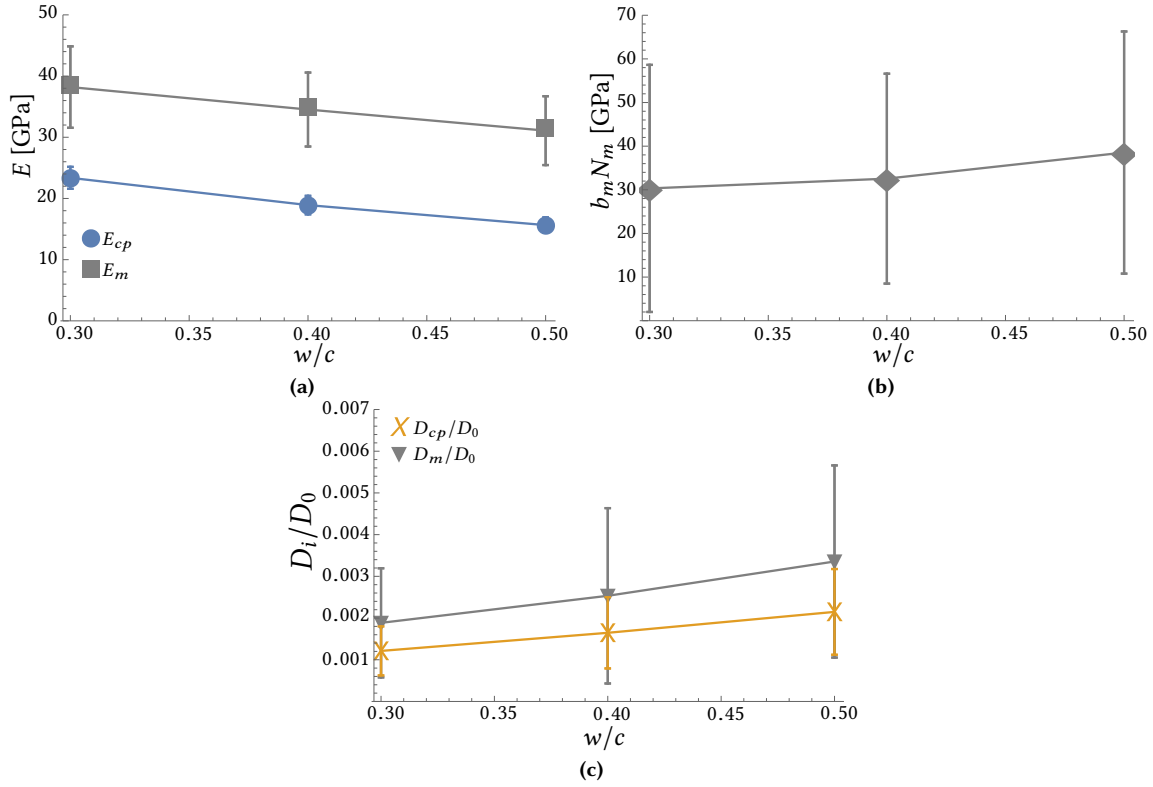
**Figure 5:** Impact of material and microstructural uncertainties on the overall effective coefficient of cement paste and mortar for three water-cement ratios: a) Young Modulus, b) Biot coefficients, and c) diffusion coefficients.

carried out.

The sensitivity analysis is based on the variance-based method. The influences of each input are measured through the Sobol indices (between 0 and 1). The first order sensitivity Sobol index, denoted $S_i$, is used to measure the sensitivity of each input parameter:

$$S_i = \frac{V_{\mathbf{x_i}}(\overline{e}(\mathbf{y}|\mathbf{x_i})}{V(\mathbf{y})}, \tag{13}$$

where $\mathbf{x_i}$ is the vector of input parameters, $\mathbf{y}$ is the output values given by the model , and $i$ defines the input index (for more details, see (Gilquin et al. 2021; Saltelli 2002)).

The system is computed using the Sobol-Saltelli method (Gilquin et al. 2021; Saltelli 2002; Venkovic et al. 2013; Sudret et al. 2010) where the Sobol indices are estimated through a Monte Carlo experiments. Let us consider $\mathbf{X}^a \in \mathbb{R}^{N^i \times N^s}$ and $\mathbf{X}^b \in \mathbb{R}^{N^i \times N^s}$ two independent input sample matrices, where $N^i$ and $N^s$ are respectively the number of input values for each model and the number of Monte Carlo samples. To compute the first order Sobol indices, a matrix, denoted $\mathbf{X}^{c,i}$, where all factors except the row $j$ is equal to $\mathbf{X}^b$, is defined for each variable. The row $i$ corresponds to the row of the matrix $\mathbf{X}^a$. The estimation of $S_i$ is obtained by the products of the vector of output values estimated from $\mathbf{X}^a$ and each matrix $\mathbf{X}^{c,i}$ ($\forall i \in N^i$) denoted respectively $\mathbf{y}^a$ and $\mathbf{y}^{c,i}$ (Gilquin et al. 2021; Saltelli 2002):

$$S_i' = \frac{\frac{1}{n}\sum_{j=1}^{n}\left(y_j^a \times y_j^{c,i}\right) - \left(\frac{1}{n}\sum_{j=1}^{n}y_j^a\right)^2}{\frac{1}{n}\sum_{j=1}^{n}\left(y_j^a\right)^2 - \left(\frac{1}{n}\sum_{j=1}^{n}y_j^a\right)^2}. \tag{14}$$

The first-order sensitivity indices measure only the direct effect of one parameter on the response of the micromechanical model. The total Sobol indices , representing the interaction effect between parameters, are estimated in the previous studies (Section 4.1 and Section 4.2). We focus here on the first order to distinguish the Sobol indices at the cement paste and at the mortar scales to highlight the highest Sobol index value. Moreover, the study allows us to consider the influence of the interaction effect of input properties on homogenized values. Only diffusive and elastic properties are considered because the Biot properties lead to high variation.

## 5.1   Analysis and results

**Young Modulus**   The Figure 6 shows the first order Sobol indices for the Young modulus of the cement paste and the mortar.

For the cement paste, the total sum of the indices is almost equal to 1, which means that there are negligible interaction effects between the morphologic and the material properties. This result confirms the conclusion of the uncertainties studies. The C-S-H  phases play a major role. The Young modulus must be estimated properly to simulate the elastic cement paste properties accurately. Furthermore, the viscoelastic properties of the cement paste, not study here, are impacted by the C-S-H  properties and volume fraction (Le 2011; Honorio et al. 2016; Sanahuja et al. 2017). The aluminate phase (here the katoite) has a greater effect than the portlandite elastic properties and other morphological properties. Note that the uncertainties could be more important for the monosulfoaluminate phases because the strength is greater than that of the katoite phase (Haeckerd et al. 2005; Socie 2019). The volume fraction uncertainties are deduced from Bogue's equation (Stutzman et al. 2014). Hydration properties based on the total concentration of aluminates (Socié et al. 2022), instead of the mass fraction of $C_3A$ (Papadakis et al. 1991; Tennis et al. 2000), could reduce the global uncertainties. The effect of other hydrates is negligible.
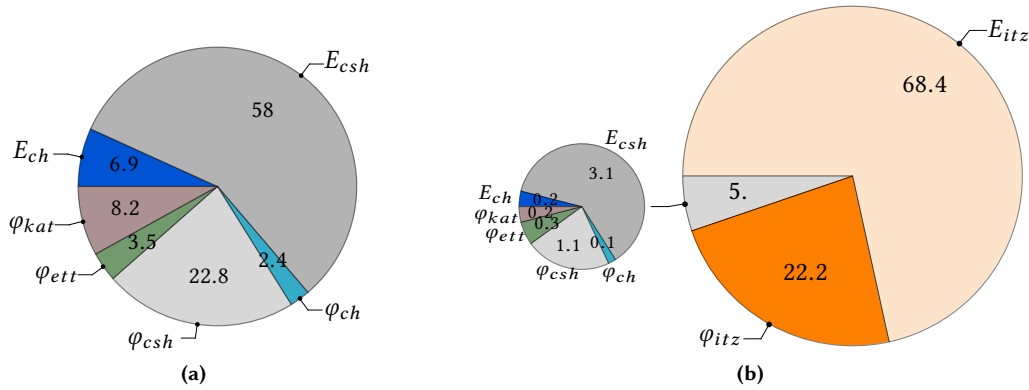


**Figure 6:** Sensitivity analysis of Young Modulus: first order Sobol indices of a) cement paste and b) mortar.

The mortar is impacted by the uncertainties associated with the ITZ phase. The total sum of the first order indices is 0.95 which highlight an impact negligible of the interaction between the variables. The main interaction is due to the ITZ strength (cf. Table 5 and Table 7). The key parameter is the ITZ Young Modulus that is hard to deduce. From an experimental point of view, the identification of the microstructural and mechanical properties of the interphase remains a challenge (Jebli et al. 2018; Salah et al. 2019; Sun et al. 2007). Numerically, the representation of the ITZ phase (Honorio et al. 2016; Stora et al. 2009) can reduce the uncertainties, but additional variations can appear due to the material representativity. Such as the hydration, adding model parameters can increase the variation (Göbel et al. 2017). Furthermore, the ITZ strength properties depend on the aggregate and sand which impact the homogenized response (Keinde 2014). Our approach seems to be a convenient choice to consider the impact of the variation of ITZ elastic properties independently to the inclusion characteristics.

**Diffusion coefficient**   The Figure 7 shows the first order Sobol indices for the diffusion coefficient of the cement paste and the mortar.

At cement paste scale, the interaction between the microstructure and the local diffusivity is negligible. The diffusivity depends essentially on the C-S-H  diffusion. This result agrees with (Patel et al. 2016). Furthermore, distinguishing the C-S-H  phases and identifying the diffusion coefficient for each phase remain an experimental challenge (Constantinides et al. 2004; Seigneur et al. 2017).

At mortar scale, the sum of the first Sobel indices highlights the main impact of the interaction term. The interaction is due to the upscaling impact of the cement paste volume fraction variation and the relationship between the ITZ and the cement paste diffusion properties. In the first order, the cement paste properties have the main effect on the homogenized coefficients. The effects of interaction and the C-S-H  properties could be one of the major roles in the multi-scale model. The mortar is also mainly impacted by the uncertainties associated with the ITZ phase (volume fraction and diffusion coefficient). The three coated homogenization scheme models the percolation of the transitional phase and thus the volume fraction is also a key parameter to estimate.

**Main results**   This study led to highlight the main sources of uncertainty of the model and the interaction of the model parameters. The interaction between the microstructure and material properties remains negligible except for the diffusion coefficient of the mortar. The main conclusion highlighted with the uncertainty study is confirmed in this study: the ITZ and C-S-H  are the main parameters that impact the efficient properties. The effect of the C-S-H  Young modulus is quite negligible at the mortar scale for the
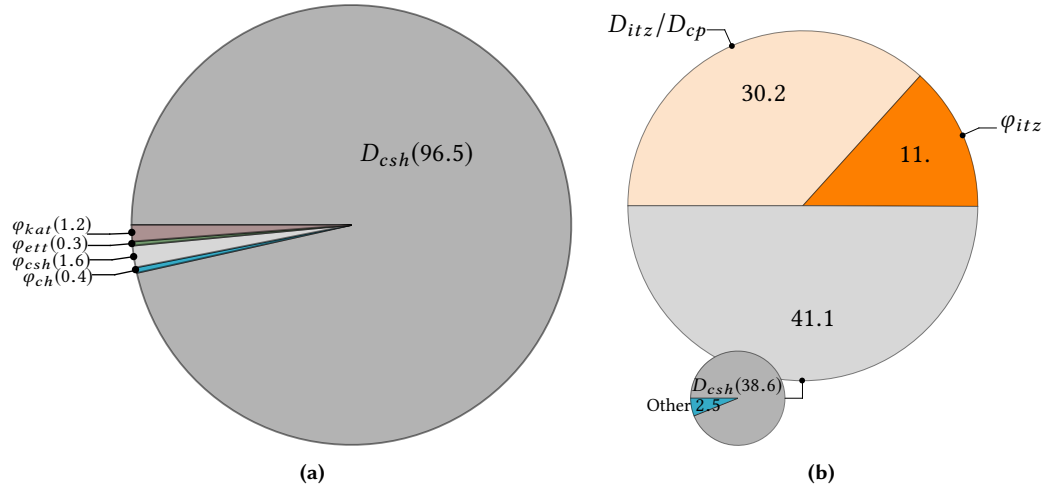
**Figure 7:** Sensitivity analysis of diffusion coefficient: first order Sobol indices of a) cement paste and b) mortar.

Young modulus compared to the ITZ parameters.

# 6   Conclusions

To study the chemo-mechanics behavior of concrete, a multi-scale microporomechanics model was proposed (Socié et al. 2022; Socié et al. 2021). The model allows to estimate the diffusive and the poroelastic properties of mortar and to highlight the effect of the microstructural characteristic. The microporomechanics model is based on representation at cement paste and mortar scales, and the homogenization scheme follows the recommendations of the literature.

The model was validated for different cement paste and mortar by comparison with analytical homogenization models and experimental results. A probabilistic approach was applied to the multi-scale model to investigate the uncertainty propagation of the microstructural and material properties. The results highlighted the main impact of the cement matrix (C-S-H) uncertainties at the cement paste scale and the Interfacial Transition Zone at the mortar scale for the diffusive and the poroelastic properties. Based on the study of (Stutzman et al. 2014), the influence of the Bogue's uncertainties through the initial volume of each hydrated was investigated. Despite the C-S-H phases, the aluminate hydrate has a major impact on the poroelastic properties. The propagation of the global uncertainties for three water-cement ratios showed the accuracy of the model to capture the effect of the material evolution on the diffusive and elastic properties. Nevertheless, the uncertainties of the Biot parameters are too important to obtain quantitative estimation.

The last part of the paper was dedicated to a sensitive analysis based on the first Sobol indices. This study highlighted the negligible interaction between the microstructure and the local diffusivity for the diffusive and elastic properties at the cement paste and for the mortar's Young Modulus. For a solid phase, the model was mainly dependent on the material properties rather than the volume fraction. For the Young Modulus, the main conclusion of the uncertainty analysis was similar. The C-S-H was the main uncertainties input parameter at the cement paste scale and the ITZ at the mortar scale. The cement paste was also impacted by the volume fraction of the aluminate phases and the effect of the portlandite phase remained negligible. For the diffusivity at the cement paste scale, the C-S-H was the main factor, in accordance with the results of (Patel et al. 2016). For the mortar diffusivity term, the interaction between the input parameters and the C-S-H effect were predominant. The study underlined the predominant impact of the ITZ volume fraction and properties to estimate mortar properties.

Finally, at cement paste, contrary to the self-consistent scheme, the Mori-Tanaka scheme does not consider directly the volume fraction of the matrix phases. At mortar scale, the role of ITZ in the overall diffusivity is still in debate (Patel et al. 2016). In that way, a major outlook of the work could be the comparison of different homogenization schemes and the evaluation of their impact on the uncertainty. Finally, the results could be applied to a chemo-mechanical Finite Element simulation to consider the impact of the overall uncertainties on the chemical and mechanical degradation kinetics.

# A   Appendices

## A.1   Uncertainties associated to the hydration model

Bogue's formula (Bogue 1952; Stutzman et al. 2014) is used to estimate the main cement phases from the clinker chemical properties. (Stutzman et al. 2014) studied the impact of the uncertainties associated with

the formula. For the authors, the uncertainties associates to the Bogue's formula have a great impact on the microstructure and material properties estimated by the hydration model. Indeed, the main cement phases $C_2S, C_3S, C_3A$ and $C_4AF$ are commonly used by hydration model to predict the initial concrete properties (Bary et al. 2014; Jennings et al. 1994; Tennis et al. 2000). To study the impact of the Bogue's formula uncertainties on the poroelastic and diffusive properties, a Monte Carlo method is carried out on the hydration model developed in (Socie 2019; Socié et al. 2022). The cement paste microstructure is estimated by a thermodynamical chemistry model under the assumption of a totally hydrated reaction (Socie 2019; Socié et al. 2022). The total concentration of each main component is estimated on the mass fraction of each component of the clinker, denoted $f_i^m$ for the solid $i$, and the water-cement mass ratio $w/c$:

$$\begin{cases} \left(C_{tot}^{aq}\right)_{Ca^{2+}} = 3C_{C_3S} + 2C_{C_2S} + 3C_{C_3A} + C_{CaSO_4} + 4C_{C_4AF} \\ \left(C_{tot}^{aq}\right)_{H_2SiO_4^{2-}} = C_{C_3S} + C_{C_2S} \\ \left(C_{tot}^{aq}\right)_{SO_4^{2-}} = C_{CaSO_4} \\ \left(C_{tot}^{aq}\right)_{Al(OH)_4^-} = 2C_{C_3A} + 2C_{C_4AF}, \end{cases} \tag{15}$$

with (Planel 2002):

$$m_{ci} = \frac{V_{total}\rho_{ci}}{\frac{w}{c}\frac{\rho_{ci}}{\rho_w} + 1}; \quad \left(C_{tot}^{aq}\right)_i = \frac{M_i f_i^m m_{ci}}{V_{total}}, \quad \forall i \in [1, 4] \tag{16}$$

where $i$ is the species, $M_i$ is the molar mass [$\text{kg mol}^{-1}$], $m_{ci}$ is the cement mass [m], $\rho_{ci}$ is the cement density [$\text{kg m}^{-3}$], $\rho_w$ is the water density [$\text{kg m}^{-3}$] and $V_{total}$ is the total volume [$\text{m}^3$].

The thermodynamic chemical solver (Socié et al. 2022; Socié et al. 2021) gives the concentration of each main phase of the cement phases and the molar fractions are simply deduced by multiplying the concentration by the molar volume. A Monte Carlo scheme is carried out on the results of (Stutzman et al. 2014) (see the Table 9) using a log-normal distribution for each phase. Furthermore, the C-S-H molar volume is hard to measure because it depends on the type of C-S-H (Tennis et al. 2000) as well as the calcium silica ratio of the phase (Stora et al. 2009). We study two values of C-S-H and the other molar volumes are summed up in the Table 10. The results are summed up in the Table 11. The solid aluminate phase, here the katoite, and the C-S-H area are impacted by the variation.

|  | $C_3S$ | $C_2S$ | $C_3A$ | $C_4AF$ | Gypsum |
|---|---|---|---|---|---|
| Mass fraction (%) | 58.4 ±9.72 | 14.5 ± 9.68 | 9.9 ± 2.6 | 7.1 ± 1.56 | 6.1 |

**Table 9:** Mass fraction used, based on the cement paste used in (Planel et al. 2006), with a water cement ratio of 0.4. The standard deviation is based on (Stutzman et al. 2014).

| Phases | Molar volume [$\text{m}^3\,\text{mol}^{-1}$] | References |
|---|---|---|
| C-S-H | 0.084, 0.078 | (Planel 2002; Lothenbach et al. 2019) |
| Portlandite | 0.033 | (Lothenbach et al. 2019) |
| Ettringite | 0.707 | (Lothenbach et al. 2019) |
| Katoite | 0.15 | (Lothenbach et al. 2019) |

**Table 10:** Molar volume of main hydrate properties.

| Phases | C-S-H | Portlandite | Ettringite | Katoite |
|---|---|---|---|---|
| Volume fraction | 0.374 ± 0.018 | 0.184 ± 0.005 | 0.144 ± 0.007 | 0.07 ± 0.011 |

**Table 11:** Results obtained by the hydration computing.

## A.2  C-S-H diffusion coefficient

The C-S-H diffusion coefficient used in the literature are summed up in the Table 12. In case of two C-S-H phases considered, the C-S-H homogenized value is estimated using the Maxwell scheme. Note that we do not include the following values $19.4 \times 10^{-12}\,\text{m}^2\,\text{s}^{-1}$ (Bogdan 2015) and $25. \times 10^{-12}\,\text{m}^2\,\text{s}^{-1}$ (Seigneur et al. 2017), because theses values are well greater than the mean value find in the literature. We find the mean and standard deviation $7.24 \pm 7.37 \times 10^{-12}$.

| Diffusion coefficient $D_{csh}$ $10^{-12}$ [m$^2$ s$^{-1}$ ] | References |
|:---:|:---:|
| 2.2 | (Bernard et al. 2012) |
| 3.2 | (Bary 2008) |
| 5.097 | (Stora et al. 2009) |
| 5.97, 1.23, 4, 2.66, 2.9 | (Patel et al. 2016) |
| 8 | (Socie 2019) |

**Table 12:** C-S-H diffusion coefficient used in the literature. In case of articles using two C-S-H phases, the homogenized value is estimated using Maxwell scheme.

## A.3 Mortar uncertainties

The section is dedicated to sum up the ITZ properties values used or measured in the literature.

| Diffusion coefficient $D_{itz}/D_{cp}$ | References |
|:---:|:---:|
| 4 | (Bogdan 2015; Kamali-Bernard et al. 2009) |
| 12.5 | (Nilenius et al. 2014) |
| 20.7 | (Patel et al. 2016) |

**Table 13:** ITZ diffusion coefficient used in the literature.

| Young Modulus $E_{itz}/E_{cp}$ | References |
|:---:|:---:|
| 0.2 | (Stora 2007) |
| 0.4 | (Heukamp 2003) |
| 0.5 | (Hashin et al. 2002; Garboczi 1997) |
| 0.66 | (Tognevi 2012) |
| 0.76 | (Honorio et al. 2016) |
| 0.74 | (Kamali-Bernard et al. 2009) |
| [0.1, 0.9] | (Keinde 2014) |

**Table 14:** ITZ Young modulus coefficient used in the literature.

| $\varphi_{itz}$ | References |
|:---:|:---:|
| 0.09 | (Bary et al. 2014) |
| 0.104 | (Stora et al. 2009) |
| 0.2 | (Honorio et al. 2016; Socie 2019) |
| 0.217 | (Stora et al. 2009) |
| 0.3 | (Heukamp 2003) |

**Table 15:** ITZ volume fraction used in the literature.

| $\phi_{itz}/\phi$ | References |
|:---:|:---:|
| [1.5, 2] | (Keinde 2014) |
| [1.5, 4] | (Kamali-Bernard et al. 2009) |
| 1.5 | (Patel et al. 2016) |

**Table 16:** ITZ porosity used in the literature.

# References

Aït-Mokhtar, A., R. Belarbi, F. Benboudjema, N. Burlion, B. Capra, M. Carcassès, J.-B. Colliat, F. Cussigh, F. Deby, F. Jacquemot, T. de Larrard, J.-F. Lataste, P. Le Bescop, M. Pierre, S. Poyet, P. Rougeau, T. Rougelot, A. Sellier, J. Séménadisse, J.-M. Torrenti, A. Trabelsi, P. Turcry, and H. Yanez-Godoy (2013). "Experimental investigation of the variability of concrete durability properties". *Cement and Concrete Research* 45, pp. 21–36. DOI: https://doi.org/10.1016/j.cemconres.2012.11.002

Bary, B. (2008). "Simplified coupled chemo-mechanical modeling of cement pastes behavior subjected to combined leaching and external sulfate attack". *International journal for numerical and analytical methods in geomechanics* 32.14, pp. 1791–1816. DOI: https://doi.org/10.1002/nag.696. eprint: https://onlinelibrary.wiley.com/doi/pdf/10.1002/nag.696

Bary, B. and S. Bejaoui (2006). "Assessment of diffusive and mechanical properties of hardened cement pastes using a multi-coated sphere assemblage model." *Cement and Concrete Research* 36.2, pp. 245–258. DOI: https://doi.org/10.1016/j.cemconres.2005.07.007

Bary, B., N. Leterrier, E. Deville, and P. Le Bescop (2014). "Coupled chemo-transport-mechanical modelling and numerical simulation of external sulfate attack in mortar". *Cement and Concrete Composites* 49, pp. 70–83. DOI: https://doi.org/10.1016/j.cemconcomp.2013.12.010

Béajoui, S., B. Bary, S. Nitsche, D. Chaudanson, and C. Blanc (2006). "Experimental and modeling studies of the link between microstructure and effective diffusivity of cement pastes". *Revue Européenne de Génie Civil* 10.9, pp. 1073–1106. DOI: 10.1080/17747120.2006.9692906

Bejaoui, S. and B. Bary (2007). "Modeling of the link between microstructure and effective diffusivity of cement pastes using a simplified composite model". *Cement and Concrete Research* 37.3, pp. 469–480. DOI: https://doi.org/10.1016/j.cemconres.2006.06.004

Bernard, F. and S. Kamali-Bernard (2012). "Predicting the evolution of mechanical and diffusivity properties of cement pastes and mortars for various hydration degrees – A numerical simulation investigation". *Computational Materials Science* 61, pp. 106 –115. DOI: https://doi.org/10.1016/j.commatsci.2012.03.023

Bogdan, M. (2015). "Morphological multisscale modeling of cementitious materials - Application to effective diffusive properties prediction." PhD thesis. École Normale Supérieur de Cachan

Bogue, R. (1952). *La chimie du ciment Portland*. Edition Eyrolles

Buffo-Lacarrière, L., A. Sellier, G. Escadeillas, and A. Turatsinze (2007). "Multiphasic finite element modeling of concrete hydration". *Cement and Concrete Research* 37.2, pp. 131–138. DOI: https://doi.org/10.1016/j.cemconres.2006.11.010

Constantinides, G. and F.-J. Ulm (2004). "The effect of two types of C-S-H on the elasticity of cement-based materials: Results from nanoindentation and micromechanical modeling". *Cement and Concrete Research.* 34.1, pp. 67–80. DOI: https://doi.org/10.1016/S0008-8846(03)00230-8

Dormieux, L., D. Kondo, and F. Ulm (2006). *MicroPoro Mechanics*. Wiley

El Hachem, R., E. Rozière, F. Grondin, and A. Loukili (2012). "Multi-criteria analysis of the mechanism of degradation of Portland cement based mortars exposed to external sulphate attack". *Cement and Concrete Research* 42.10, pp. 1327–1335. DOI: https://doi.org/10.1016/j.cemconres.2012.06.005

Gallé, C., H. Peycellon, and P. Le Bescop (2004). "Effect of an accelerated chemical degradation on water permeability and pore structure of cementbased materials". *Advances in Cement Research* 16.3, pp. 105–114. DOI: https://doi.org/10.1680/adcr.2004.16.3.105

Garboczi, E.-J. and D.-P. Bentz (1997). "Analytical formulas for interfacial transition zone properties". *Advanced Cement Based Materials* 6.3, pp. 99–108. DOI: https://doi.org/10.1016/S1065-7355(97)90016-X

Garboczi, E. (1997). "Stress, displacements, and expansive cracking around a single spherical aggregate under different expansive conditions". *Cement and Concrete Research* 27.4, pp. 495 –500

Gilquin, L., C. Prieur, E. Arnaud, and H. Monod (2021). "Iterative estimation of Sobol' indices based on replicated designs." *Comp. Appl. Math.* 40.18. DOI: https://doi.org/10.1007/s40314-020-01402-5

Göbel, T., T. Lahmer, and A. Osburg (2017). "Uncertainty analysis in multiscale modeling of concrete based on continuum micromechanics". *European Journal of Mechanics - A/Solids* 65, pp. 14–29. DOI: https://doi.org/10.1016/j.euromechsol.2017.02.008

Haeckerd, C.-J, E. Garboczi, J. Bullard, R. Bohn, Z. Sun, S. Shah, and T. Voigt (2005). "Modeling the linear elastic properties of Portland cement paste". *Cement and Concrete Research* 35.10, pp. 1948–1960. DOI: https://doi.org/10.1016/j.cemconres.2005.05.001

Hashin, Z. and P. Monteiro (2002). "An inverse method to determine the elastic properties of the interphase between the aggregate and the cement paste". *Cement and Concrete Research* 32.8, pp. 1291–1300. DOI: https://doi.org/10.1016/S0008-8846(02)00792-5

Heukamp, F. (2003). "Chemomechanics of Calcium Leaching of Cement-Based Materials at Different Scales: The Role of CH-Dissolution and C-S-H-Degradation on Strength and Durability Performance of Materials and Structures." PhD thesis. Massachussetts Institute of Technology

Honorio, T., B. Bary, and F. Benboudjema (2016). "Multiscale estimation of ageing viscoelastic properties of cement-based materials: A combined analytical and numerical approach to estimate the behaviour at

early age." *Cement and Concrete Research* 85, pp. 137–155. DOI: https://doi.org/10.1016/j.cemconres.2016.03.010

Jebli, M., F. Jamin, E. Malachanne, E. GarciaDiaz, and M. El Youssoufi (2018). "Experimental characterization of mechanical properties of the cement-aggregate interface in concrete." *Construction and Building Materials* 161, pp. 16–25

Jennings, H. and P. Tennis (1994). "Model for the Developing Microstructure in Portland Cement Pastes". *Journal of the American Ceramic Society* 77.12, pp. 3161–3172. DOI: https://doi.org/10.1111/j.1151-2916.1994.tb04565.x. eprint: https://ceramics.onlinelibrary.wiley.com/doi/pdf/10.1111/j.1151-2916.1994.tb04565.x

Kamali-Bernard, S., F. Bernard, and W. Prince (2009). "Computer modelling of tritiated water diffusion test for cement based materials". *Computational Materials Science* 45.2, pp. 528–535. DOI: https://doi.org/10.1016/j.commatsci.2008.11.018

Keinde, D. (2014). "Etude du béton à l'échelle mesoscopique : simulation numérique et tests de micro-indentation". PhD thesis. INSA Rennes

Le, T. (2011). "Modélisation multi-échelle des matériaux viscoélastiques hétérogènes : application à l'identification et à l'estimation du fluage propre d'enceintes de centrales nucléaires." PhD thesis. Université Paris-Est

Le Bellego, C. (2001). "Couplages chimiemécanique dans les structures en béton attaquées par l'eau: Etude expérimentale et analyse numérique". PhD thesis. Ecole Normale Supérieure de Cachan

Lothenbach, B., A. Dmitrii, D. Kulik, T. Matschei, M. Balonis, L. Baquerizo, B. Dilnesa, D. Miron, and R. Myers (2019). "Cemdata18: A chemical thermodynamic database for hydrated Portland cements and alkali-activated materials". *Cement and Concrete Research* 115, pp. 472–506. DOI: https://doi.org/10.1016/j.cemconres.2018.04.018

Mori, T. and K. Tanaka (1973). "Average stress in matrix and average elastic energy of materials with misfitting inclusions". *Acta Metallurgica* 21.5, pp. 571–574. DOI: https://doi.org/10.1016/0001-6160(73)90064-3

Nguyen, N., A. Giraud, and D. Grgic (2011). "A composite sphere assemblage model for porous oolitic rocks". *International Journal of Rock Mechanics and Mining Sciences* 48.6, pp. 909–921. DOI: https://doi.org/10.1016/j.ijrmms.2011.05.003

Nguyen, T. (2010). "Apport de la modélisation mésoscopique dans la prédiction des écoulements dans les ouvrages en béton fissuré en conditions d'accident grave". PhD thesis. Université de Pau et des Pays de l'Adour

Nilenius, F., F. Larsson, K. Lundgren, and K. Runesson (2014). "Computational homogenization of diffusion in three-phase mesoscale concrete". *Computational Mechanics* 54, pp. 461 –472. DOI: https://doi.org/10.1007/s00466-014-0998-0

Papadakis, V., C. Vayenas, and M. Fardis (1991). "Physical and Chemical Characteristic Affecting the Durability of Concrete". *American Concrete Institute Material Journal* 2.88, pp. 186–196

Patel, R., Q. Phung, S. Seetharam, J. Perko, D. Jacques, N. Maes, G. De Schutter, G. Ye, and K. Van Breugel (2016). "Diffusivity of saturated ordinary Portland cement-based materials: A critical review of experimental and analytical modelling approaches". *Cement and Concrete Research* 90, pp. 52–72. DOI: https://doi.org/10.1016/j.cemconres.2016.09.015

Planel, D. (2002). "Les effets couplés de la précipitation d'espèces secondaires sur le comportement mécanique et la dégradation chimique des Bétons". PhD thesis. Université de Marne la Vallée

Planel, D., J. Sercombe, P. Le Bescop, F. Adenot, and J.-M. Torrenti (2006). "Long-term performance of cement paste during combined calcium leaching–sulfate attack: kinetics and size effect". *Cement and Concrete Research* 36.1, pp. 137–143. DOI: https://doi.org/10.1016/j.cemconres.2004.07.039

Salah, N., M. Jebli, E. Malachanne, F. Jamin, F. Dubois, A.-S. Caro, E. Garcia-Diaz, and M. S. El Youssoufi (2019). "Identification of a cohesive zone model for cement paste-aggregate interface in a shear test." *European Journal of Environmental and Civil Engineering*, pp. 1–15. DOI: 10.1080/19648189.2019.1623082

Saltelli, A. (2002). "Making best use of model evaluations to compute sensitivity indices". *Computer Physics Communications* 145.2, pp. 280–297. DOI: https://doi.org/10.1016/S0010-4655(02)00280-1

Sanahuja, J. and S. Huang (2017). "Mean-Field Homogenization of Time-Evolving Microstructures with Viscoelastic Phases: Application to a Simplified Micromechanical Model of Hydrating Cement Paste". *Journal of Nanomechanics and Micromechanics* 7.1, p. 04016011. DOI: 10.1061/(ASCE)NM.2153-5477.0000116

Seigneur, N., E. L'Hôpital, A. Dauzères, J. Sammaljavi, M. Voutilainen, P. Labeau, A. Dubus, and V. Detilleux (2017). "Transport properties evolution of cement model system under degradation - Incorporation of a pore-scale approach into reactive transport modelling". *Physics and Chemistry of the Earth, Parts A/B/C* 99. Mechanisms and Modelling of Waste-Cement and Cement-Host Rock Interactions, pp. 95–109. DOI: https://doi.org/10.1016/j.pce.2017.05.007

Socie, A. (2019). "Modélisation chimiomécanique de la fissuration de matériaux cimentaires : vieillissement et tenue des enceintes de confinement des centrales nucléaires." PhD thesis. Université de Montpellier

Socié, A., F. Dubois, Y. Monerie, and F. Perales (2021). "Multibody approach for reactive transport modeling in discontinuous-heterogeneous porous media." *Computational Geosciences.* Pp. 1473–1491. DOI: https://doi.org/10.1007/s10596-021-10058-x

Socié, A., F. Dubois, Y. Monerie, M. Neji, and F. Perales (2022). "Simulation of internal and external sulfate attacks of concrete with a generic reactive transport-poromechanical model." *European Journal of Environmental and Civil Engineering.* Under review

Stora, E. (2007). "Multiscale modelling and simulations of the chemo-mechanical behavior of degraded cementbased materials". PhD thesis. Université ParisEst

Stora, E., B. Bary, Q.-C. He, E. Deville, and P. Montarnal (2009). "Modelling and simulations of the chemo–mechanical behaviour of leached cement-based materials: Leaching process and induced loss of stiffness". *Cement and Concrete Research* 39.9, pp. 763–772. DOI: https://doi.org/10.1016/j.cemconres.2009.05.010

Stutzman, P., A. Heckert, A. Tebbe, and S. Leigh (2014). "Uncertainty in Bogue-calculated phase composition of hydraulic cements". *Cement and Concrete Research* 61-62, pp. 40–48. DOI: https://doi.org/10.1016/j.cemconres.2014.03.007

Sudret, B., T. Yalamas, E. Noret, and P. Willaume (2010). "Sensitivity analysis of nested multiphysics models using polynomial chaos expansions". Safety,Reliability and Risk of Structures, Infrastructures and Engineering Systems (Osaka, Japan). Furuta, Frangopol & Shinozuka, pp. 3883–3890

Sun, Z., E. Garboczi, and S. Shah (2007). "Modeling the elastic properties of concrete composites: Experiment, differential effective medium theory, and numerical simulation". *Cement and Concrete Composites* 29.1, pp. 22–38. DOI: https://doi.org/10.1016/j.cemconcomp.2006.07.020

Tennis, P. and H. Jennings (2000). "A model for two types of calcium silicate hydrate in the microstructure of Portland cement pastes". *Cement and Concrete Research* 30.6, pp. 855–863. DOI: https://doi.org/10.1016/S0008-8846(00)00257-X

Tognevi, A. (2012). "Modélisation multi-échelle et simulation du comportement thermo-hydro-mécanique du béton avec représentation explicite de la fissuration." PhD thesis. École Normale Supérieure de Cachan

Ulm, J.-F., G. Constantinides, and F. Heukamp (2004). "Is concrete a poromechanics material?- A multiscale investigation of poroelastic properties". *Materials and Structures* 37, pp. 43 –58. DOI: https://doi.org/10.1007/BF02481626

Venkovic, N., L. Sorelli, B. Sudret, T. Yalamas, and R. Gagné (2013). "Uncertainty propagation of a multiscale poromechanics-hydration model for poroelastic properties of cement paste at early-age". *Probabilistic Engineering Mechanics* 32, pp. 5–20. DOI: https://doi.org/10.1016/j.probengmech.2012.12.003